Journal of Visualized Experiments

3D Cell-Printed Hypoxic Cancer-on-a-Chip for Recapitulating Pathologic Progression of Solid Cancer

--Manuscript Draft--

Article Type:	Invited Methods Collection - JoVE Produced Video
Manuscript Number:	JoVE61945R2
Full Title:	3D Cell-Printed Hypoxic Cancer-on-a-Chip for Recapitulating Pathologic Progression of Solid Cancer
Corresponding Author:	Hee-Gyeong Yi, Ph.D. Chonnam National University Gwangju, Gwangju KOREA, REPUBLIC OF
Corresponding Author's Institution:	Chonnam National University
Corresponding Author E-Mail:	hgyi@jnu.ac.kr
Order of Authors:	Wonbin Park
	Mihyeon Bae
	Minseon Hwang
	Jinah Jang
	Dong-Woo Cho
	Hee-Gyeong Yi, Ph.D.
Additional Information:	
Question	**Response**
Please specify the section of the submitted manuscript.	Bioengineering
Please indicate whether this article will be Standard Access or Open Access.	Standard Access (US$2,400)
Please indicate the **city, state/province, and country** where this article will be **filmed**. Please do not use abbreviations.	Pohang, Gyeongbuk, Korea
Please confirm that you have read and agree to the terms and conditions of the author license agreement that applies below:	I agree to the Author License Agreement
Please provide any comments to the journal here.	Wonbin Park and Mihyeon Bae are the first authors. Jinah Jang, Dong-Woo Cho, and Hee-Gyeong Yi are the corresponding authors.

TITLE:

3D Cell-Printed Hypoxic Cancer-on-a-Chip for Recapitulating Pathologic Progression of Solid Cancer

AUTHORS AND AFFILIATIONS:

Wonbin Park[1*], Mihyeon Bae[1*], Minseon Hwang[1], Jinah Jang[2†], Dong-Woo Cho[1], Hee-Gyeong Yi[1,3]

[1]Department of Mechanical Engineering, Pohang University of Science and Technology (POSTECH), Pohang, Korea
[2]Department of Creative IT Engineering, Pohang University of Science and Technology (POSTECH), Pohang, Korea
[3]Department of Rural and Biosystems Engineering, College of Agriculture and Life Sciences, Chonnam National University, Gwangju, Korea

*These authors contributed equally.

Email addresses of co-authors:

Wonbin Park (wbpark@postech.ac.kr)
Mihyeon Bae (bmh0627@postech.ac.kr)
Minseon Hwang (mshwang@postech.ac.kr)
Jinah Jang (jinahjang@postech.ac.kr)
Dong-Woo Cho (dwcho@postech.ac.kr)
Hee-Gyeong Yi (hgyi@jnu.ac.kr)

Co-corresponding authors:

Jinah Jang (jinahjang@postech.ac.kr)
Dong-Woo Cho (dwcho@postech.ac.kr)
Hee-Gyeong Yi (hgyi@jnu.ac.kr)

KEYWORDS:

3D cell-printing, 3D microphysiological system, organ-on-a-chip, solid cancer, microenvironment, hypoxia, oxygen gradient, pathology

SUMMARY:

Hypoxia is a hallmark of tumor microenvironment and plays a crucial role in cancer progression. This article describes the fabrication process of a hypoxic cancer-on-a-chip based on 3D cell-printing technology to recapitulate a hypoxia-related pathology of cancer.

ABSTRACT:

Cancer microenvironment has a significant impact on the progression of the disease. In particular, hypoxia is the key driver of cancer survival, invasion, and chemoresistance. Although several in vitro models have been developed to study hypoxia-related cancer pathology, the complex interplay of the cancer microenvironment observed in vivo has not been reproduced yet owing to the lack of precise spatial control. Instead, 3D biofabrication approaches have been

proposed to create microphysiological systems for better emulation of cancer ecology and accurate anticancer treatment evaluation. Herein, we propose a 3D cell-printing approach to fabricate a hypoxic cancer-on-a-chip. The hypoxia-inducing components in the chip were determined based on a computer simulation of the oxygen distribution. Cancer-stroma concentric rings were printed using bioinks containing glioblastoma cells and endothelial cells to recapitulate a type of solid cancer. The resulting chip realized central hypoxia and aggravated malignancy in cancer with the formation of representative pathophysiological markers. Overall, the proposed approach for creating a solid-cancer-mimetic microphysiological system is expected to bridge the gap between in vivo and in vitro models for cancer research.

INTRODUCTION:

The cancer microenvironment is a critical factor driving cancer progression. Multiple components, including biochemical, biophysical, and cellular cues, determine the pathological features of cancer. Among these, hypoxia is strongly associated with cancer survival, proliferation, and invasion[1]. Due to the unlimited growth and division of cancer cells, nutrients and oxygen are continuously depleted, and a hypoxic gradient is generated. Under low-oxygen conditions, cells activate hypoxia-inducible transcription factor (HIF)-associated molecular cascade. This process induces a necrotic core, triggers metabolic changes, and initiates blood vessel hyperplasia and metastasis[2,3]. Subsequently, hypoxia in cancer cells causes the destruction of neighboring normal tissues. Furthermore, hypoxia is strongly associated with the therapeutic resistance of solid tumors in multifactorial manners. Hypoxia may severely impede radiotherapy, as radiosensitivity is limited owing to reactive oxygen species[1,4]. In addition, it decreases pH levels of cancer microenvironments, which decreases drug accumulation[1]. Therefore, reproducing pathological features related to hypoxia in vitro is a promising strategy for scientific and pre-clinical findings.

Modeling a specific microenvironment of cancer is essential for understanding cancer development and exploring appropriate treatments. Although animal models have been widely used because of their strong physiological relevance, issues related to species differences and ethical problems exist[5]. Furthermore, although conventional 2D and 3D models allow for the manipulation and real-time imaging of cancer cells for an in-depth analysis, their architectural and cellular complexity cannot be fully recapitulated. For example, cancer spheroid models have been widely used, as cancer cell aggregation in a spheroid can naturally generate hypoxia in the core. Moreover, large numbers of cellular spheroids of uniform size have been produced using plastic- or silicone-based multi-well systems[6,7]. However, the lower flexibility with regard to capturing the exact heterogeneous structure of cancerous tissues with conventional platforms has required the establishment of an advanced biofabrication technology to build a highly biomimetic platform to improve cancer research[8].

3D microphysiological systems (MPSs) are useful tools to recapitulate the complex geometry and pathological progression of cancer cells[9]. As cancer cells sense the biochemical gradient of growth factors and chemokines and the mechanical heterogeneity reproduced on the system, important features of cancer development can be investigated in vitro. For instance, cancer viability, metastatic malignancy, and drug resistance depending on the varying oxygen concentrations has been studied using MPSs[10,11]. Despite recent advancements, generating

hypoxic conditions of in vitro models relies on complex fabrication procedures, including connection with physical gas pumps. Therefore, simple, and flexible methods to build cancer-specific microenvironments are needed.

3D cell printing technology has gained considerable attention because of its precise control of the spatial arrangement of biomaterials to recapitulate native biological architectures[12]. In particular, this technology overcomes the existing limitations of 3D hypoxia models owing to its high controllability and feasibility for building the spatial features of the cancer microenvironment. 3D printing also facilitates computer-aided manufacturing through a layer-by-layer process, thereby providing a rapid, accurate, and reproducible construction of complex geometries to mimic actual tissue architectures. In addition to the advantages of existing manufacturing strategies for 3D MPSs, the pathophysiological features of cancer progression can be reproduced by patterning the biochemical, cellular, and biophysical components[13,14].

Herein, we present a 3D cell-printing strategy for a hypoxic cancer-on-a-chip for recapitulating the heterogeneity of a solid cancer (**Figure 1**)[15]. The fabrication parameters were determined via a computational simulation of central hypoxia formation in the system. Cancer-stroma concentric rings were printed using collagen bioinks containing glioblastoma cells and endothelial cells to emulate the pathophysiology of glioblastoma, a type of solid cancer. The formation of a radial oxygen gradient aggravated cancer malignancy, indicating strengthened aggressiveness. Furthermore, we indicate future perspectives for the applications of the chip to patient-specific preclinical models. The proposed approach for creating a solid-cancer-mimetic microphysiological system is expected to bridge the gap between in vivo and in vitro models of cancer.

PROTOCOL:

1. Computer simulation of oxygen gradient formation

1.1. Generation of a 3D geometry model for hypoxic cancer-on-a-chip printing

1.1.1. Run a 3D CAD software.

1.1.2. Sketch the geometry model of hypoxic cancer-on-a-chip. Click on **Sketch** and select the desired plane to draw the geometry. Refer to the drawing (**Figure 2A**) for the detail scale of each part.

1.1.3. Set the thickness of the geometry by clicking on **Feature-Protrusion Boss/Base**. Enter the desired thickness (refer to **Figure 2A**) in the empty box and select the green check icon to form the 3D geometry.

NOTE: The dimension of the cancer-on-a-chip is defined based on the desired volumes of media and hydrogel. In the present experiment, the desired volumes of media and hydrogel were approximately 1,500 μL and 500 μL, respectively, based on the previous practical experiences for

resolution of extrusion-based bioprinter.

1.1.4. Save the geometry file as a 3D CAD file format (.prt or .stl).

1.2. Determination of cellular density for induction of hypoxic core

1.2.1. Run a physical diffusion simulation program.

1.2.2. Click on **LiveLink** and select the CAD program used. Click on **Synchronize** to import the geometry of the hypoxic cancer-on-a-chip on the simulation program. As the inner space of the chamber will be filled with a culture medium in an actual experimental setting, oxygen will diffuse across the inner space of the chamber and the cellular construct, which will be composed of cell-laden hydrogels.

NOTE: Refer to previous study for details on the physical parameters[15].

1.2.3. Define the imported 3D geometry as a control volume of the space wherein oxygen diffuses, and the cells consume oxygen (**Figure 2B**).

1.2.4. Run a computer analysis for gas diffusion analysis following a user guide and previously established methods[16,17].

1.2.5. From the computer analysis results, export the estimated oxygen concentration data over cross-section A-A' at each time point following the user guide. The governing equation is based on Fick's first law, as expressed in Eq. (1) (**Figure 2C**).

$$\frac{\partial c}{\partial t} + \nabla \cdot (-D\nabla c) = -N_{cell}\frac{V_{O_2,max}c}{K_m+c}, \qquad (1)$$

where *c* is the concentration, *D* is the oxygen diffusion coefficient, N_{cell} is the density of the cells, $V_{O_2,max}$ is the maximum up-take rate of oxygen, and K_m is the Michaelis–Menten constant. The constants were applied as described in a previous publication[15].

NOTE: Each time point means a step point to observe oxygen diffusion change over time.

1.2.6. Evaluate whether the minimal oxygen level reaches a threshold of hypoxia and repeat the computer analysis process with an increment or decrement of cellular density.

NOTE: Define that hypoxia gradient is formed in the construct if the oxygen level of 80% in the hydrogel area is less than 0.02 mM after 24 h.

1.2.7. Confirm the number of cells required to generate the oxygen gradient inducing hypoxia in the central region from Fick's first law in step 1.2.5 and the simulation results from step 1.2.6.

NOTE: In this protocol, cell number was 2×10^6cells/each construct.

2. Cell culture of cancer cells and stromal cells

2.1. Preparation of cell culture media to avoid physiological stress

2.1.1. For U-87 MG cells (immortalized human glioblastoma cell line), place 12 mL of high-glucose Dulbecco's modified Eagle medium containing 10% fetal bovine serum, 100 U/mL penicillin, and 100 µg/mL streptomycin in a T-75 cell culture flask in a 37 °C, 5% CO_2 humidified incubator for 30 min to minimize the thermal and alkaline effects of the medium on the cells.

NOTE: Glioblastoma was chosen as a type of solid cancer because it has aggressive characteristics in a hypoxic environment. Other various types of cancers can be applied to this model.

2.1.2. For human umbilical vein endothelial cells (HUVECs), place 12 mL of endothelial cell growth medium in a T-75 cell culture flask in a 5% CO_2 humidified incubator at 37 °C for 30 min.

NOTE: HUVECs were chosen because it is one of the most representative endothelial cell lines. Various types of stromal cells can also be applied to this model.

2.2. Rapid thawing of cryopreserved cancer cells and stromal cells and their maintenance

2.2.1. Move cryovials containing 5 x 10^5 U-87 MG cells and HUVECs from the liquid nitrogen container to a laminar flow cabinet. Immediately loosen and retighten the cap to release the internal pressure.

2.2.2. Gently place the cryopreserved cells in a water bath at 37 °C for 2 min, keeping the cap out of the water. Rinse the vials with 70% ethanol under laminar flow to prevent contamination.

2.2.3. Transfer the thawed cells to the flasks containing the prepared cell culture media described in step 2.1 and place the cell-containing flasks in a 5% CO_2 humidified incubator at 37 °C for cell recovery.

2.2.4. Refresh the cell culture media every 2 days and maintain the cell growth.

2.2.5. After 24 h of thawing, replace the cell culture media to avoid cytotoxicity of dimethyl sulfoxide (DMSO), which was used for cell freezing. Use HUVECs, which has undergone less than 6 passages.

3. Preparation of collagen pre-gel solution

3.1. Solubilization of collagen sponge with 0.1 N hydrochloric acid (HCl)

3.1.1. Prepare a solution of 0.1 N HCl and filter it with a 0.2 µm syringe filter.

3.1.2. For 3 mL of a 1% (w/v) neutralized collagen pre-gel solution, prepare collagen sponges cut into 5 x 5 mm^2 pieces and weighing 30 mg.

3.1.3. Transfer the cut collagen pieces to a sterile 10 mL glass vial.

NOTE: Prepare 1.5 times volume of the required collagen hydrogel, considering the loss of the hydrogel due to the sticky characteristic of the collagen solution.

3.1.4. Add 2.4 mL of 0.1 N HCl into the collagen-containing glass vial and incubate it on the rocker at 15 rpm and 4 °C for 3 days.

NOTE: The volume of the 0.1 N HCl solution was four-fifths of the final volume of required collagen hydrogel. In this case, 3 mL of collagen was prepared.

3.1.5. After digestion, sieve the undigested collagen particles using a 40 µm cell strainer. Store the acidic collagen solution at 4 °C and use within 7 days.

3.2. pH adjustment for 1% neutralized collagen pre-gel solution

3.2.1. Centrifuge the acidic collagen solution at 516 x *g* for 5 min at 4 °C.

3.2.2. Add 30 µL of phenol red solution as a pH indicator to a final concentration of 1% (v/v) and 300 µL of 10x phosphate-buffered saline (PBS) buffer to a final concentration of 10% (v/v) in the collagen pre-gel solution.

3.2.3. Neutralize the pH to 7 with 1 N sodium hydroxide (NaOH), verifying the color change.

NOTE: Based on the formula, moles H^+ = molarity H^+ x volume H^+ = moles OH^-= molarity OH^- x volume OH^-, add 240 µL of NaOH.

3.2.4. Add distilled water to obtain a total volume of 3 mL.

3.2.5. After pH adjustment, store the 1% (w/v) neutralized collagen pre-gel solution at 4 °C and use within 3 days.

NOTE: To precheck the gelation of the neutralized collagen pre-gel solution, make 50 µL collagen droplets on a small dish using a positive displacement pipette and incubate them in a 37 °C incubator for 1 h. Refer to the following three methods to verify the cross-linking of collagen droplets.

3.2.6. Check whether the color of collagen has changed into opaque white from transparent color.

3.2.7. Tilt the container and check whether the collagen is adhered to the bottom of the container.

3.2.8. Pour 1x PBS on the droplets and check whether the collagen construct is not broken in the solution.

4. 3D printing of gas-permeable barrier

4.1. 3D printing of a sacrificial poly (ethylene-vinyl acetate) (PEVA) mold

4.1.1. Generate the 3D geometry of the sacrificial PEVA mold defined in step 1 using a 3D CAD software (**Figure 3A**).

NOTE: The 3D geometry and detailed model scale including dimension, units, and line types were shown in **Figure 2A**.

4.1.2. Convert the 3D CAD file into an STL file format by clicking on **File | Save-File type as STL**. Also, click on **Option | Output form as ASCII** for G-code generation.

4.1.3. Click on **File | Open STL file** and select the saved STL file to import the generated STL file. Click on **Slice model** of STL-CAD exchanger to automatically generate the G-code of the sacrificial PEVA mold (**Figure 3B,C**).

NOTE: The printing path is generated with the connection of intersected points between the fundamental figure of the STL file and the slicing plane (i.e., layer). Basically, the fundamental figure of a fragment in an STL file is a triangle that contains the 3D coordinates. After the intersected points between the triangle and the layer are obtained, a G-code for printing is generated by connecting each point without an overlapped path on a layer[18]. Any G-code generation algorithm on board software can be used to generate printing paths for the chip fabrication.

4.1.4. Prepare a sterile adhesive and hydrophilic histology slide.

NOTE: The hydrophilic slide glass is critical for the permanent bonding of polydimethylsiloxane (PDMS) on the glass and the adhesion of the collagen constructs encapsulating cancer cells and stromal cells.

4.1.5. Print the sacrificial PEVA mold on the slide with a 50 G precision nozzle at a pneumatic pressure of 500 kPa at 110 °C.

NOTE: The line width is affected by the feed rate, nozzle gauge, and temperature of the material. The 50 G nozzle was used and a feed rate of 400 was applied to generate 500 µm line width for the sacrificial wall. The nozzle gauge, pneumatic pressure, and feed rate are defined with practical results[19]. The sacrificial wall needs to be sufficiently thick to hold the PDMS solution,

which is the next fabrication step.

4.2. Casting of polydimethylsiloxane (PDMS) barrier

4.2.1. Mix 6 mL PDMS base elastomer and 0.6 mL curing agent homogenously over 5 min in a plastic reservoir. This can fabricate 6 hypoxic cancer-on-chips, considering the loss due to the sticky characteristic of PDMS.

4.2.2. Load the blended PDMS solution into a 10 mL disposable syringe and fit the syringe head with a 20 G plastic tapered dispense tip.

4.2.3. Fill the sacrificial PEVA mold with the blended PDMS solution in the syringe. The blended PDMS will fill the sacrificial PEVA mold with a convex surface. The height of the PDMS barrier will be higher than that of the PEVA mold.

4.2.4. Cure the PDMS barrier in an oven at 40 °C for over 36 h to avoid the melting of PEVA. Do not increase the temperature to over 88 °C, which is the melting temperature of PEVA.

4.2.5. Detach the sacrificial PEVA mold with a pair of precision tweezers and sterilize the gas-permeable barrier at 120 °C in an autoclave.

5. Preparation of cell-encapsulated collagen bio-inks

5.1. Detachment of the prepared cancer cells and stromal cells

NOTE: Considering cell viability, the entire printing process should be completed as soon as possible after detaching the cells.

5.1.1. Wash cancer and stromal cells with 10 mL of 1x PBS using a serological pipette; treat with 2 mL of 0.25% trypsin-ethylenediaminetetraacetic acid (EDTA) using a pipette and incubate them for 3 min at 37 °C.

5.1.2. Neutralize the trypsinized cells with 3 mL of cell culture media; collect the suspensions of cells into 15 mL conical tubes and centrifuge at 516 x *g* for 5 min at 20 °C.

5.1.3. Aspirate the supernatant slowly; resuspend the cell pellets in 5 mL cell culture media and count the number of cells using a hemocytometer.

5.1.4. Transfer 5 x 10^6 cells of each cell type into new 15 mL conical tubes and centrifuge them at 516 x *g* for 5 min at 20 °C.

5.1.5. Aspirate the supernatant off and place it on wet ice.

5.2. Mixing of each cell type with the 1% neutralized collagen pre-gel solution

NOTE: To avoid thermal solidification of the 1% neutralized collagen pre-gel solution, this process should be performed on wet ice.

5.2.1. Resuspend each type of cell pellet collected in step 5.1.4 with 20 µL of cell culture media each.

5.2.2. Add 1 mL of the 1% neutralized collagen pre-gel solution into each of the resuspended cell suspensions and mix them homogenously using a positive displacement pipette. The final concentration of each cell type will be 5 x 10^6 cells/mL.

5.2.3. Transfer the cell-encapsulated collagen bioinks into 3 mL disposable syringes using a positive disposable pipette and store the syringes at 4 °C until 3D cell-printing.

6. 3D cell-printing of cancer-stroma concentric rings

6.1. 3D cell-printing of collagen bioinks encapsulating cancer cells and stromal cells

6.1.1. Generate the 3D geometry of the cancer-stroma concentric rings defined in step 1.2 using a 3D CAD software.

NOTE: The dimensions of the cancer stroma concentric rings are defined via simulated parameters. The final dimension parameter dimensions are shown in **Figure 3A**.

6.1.2. Convert the 3D CAD file into an STL file format and generate a G-code of the cancer-stroma concentric rings using a STL-CAD exchanger.

NOTE: Refer to the note in step 4.1.2 for the G-code generation algorithm.

6.1.3. Load the cell-encapsulated collagen bioinks contained in 3 mL disposable syringes to the head of the 3D printer and set the temperature of the head and plate to 15 °C.

NOTE: If the temperature of the head and plate of the printer reaches over 37 °C, the bioink gets cross-linked and no longer prints.

6.1.4. Load the generated printing path on the control software of the 3D printer.

6.1.5. By clicking on the **Start** button, print the collagen bioinks encapsulating cancer cells and stromal cells on the gas-permeable barrier following the loaded G-code with an 18 G plastic needle at pneumatic pressure of approximately 20 kPa at 15 °C.

6.1.6. At the end of every printing operation, manually place a sterilized 22 mm x 50 mm glass cover on top of the gas-permeable barrier to generate the hypoxic gradient.

NOTE: Compare two groups depending on the presence of glass cover (GR+) and absence (GR-) of that to verify the generation of the hypoxic gradient.

6.1.7. After generating three hypoxic cancer-on-chips, transfer the chips to an incubator at 37 °C for 1 h to cross-link the collagen bioinks.

6.2. Completion of the fabrication process and maintenance of the hypoxic cancer-on-a-chip

6.2.1. After completion of all 3D cell-printing processes of the hypoxic cancer-on-a-chip, gently rub the cover glasses on top of the gas-permeable barriers with the cell-scrapper for tight bonding (**Figure 4A,B**).

NOTE: The cover glass and the gas-permeable barrier are assembled via hydrophobic bonding without chemical glues, simply scraping the bonded part between the cover glass and the PDMS barrier.

6.2.2. Introduce 1.5 mL of endothelial cell growth medium to each chip. To avoid detachment of the cancer construct, introduce cell culture medium from one side of the chip. Tilt the chip to allow the cell culture media to flow using a pipette.

6.2.3. Refresh the cell culture media every day for a week. Use a pipette to aspirate the cell culture medium; do not use a pressure pump.

7. Evaluation of post-printing cell viability

7.1. Preparation of samples and treatment with calcein AM and EthD-1 solution

7.1.1. Warm 1x PBS in a water bath at 37 °C.

7.1.2. Prepare the assay solution by adding 0.75 µL of calcein acetoxymethyl (calcein AM) and 3 µL of ethidium homodimer (EthD-1) to 1.5 mL pre-warmed PBS.

7.1.3. Carefully aspirate all media from the chip using a pipette.

7.1.4. Wash the cancer construct with prewarmed PBS. Fill 1.5 mL PBS into the chip using a pipette and let it stand for 10 min at room temperature. To avoid deformation of the cancer construct, introduce 1x PBS from one side of the chips and tilt the chips to allow 1x PBS to flow.

7.1.5. Aspirate the PBS from the chip; treat the 1.5 mL assay solution and incubate the chip at 37 °C for 20 min using a foil to protect from light. Use a pipette to aspirate 1x PBS; do not use a pressure pump.

7.2. Imaging of the cell viability using a fluorescence microscope

7.2.1. View and capture the labeled cells using a fluorescence microscope (**Figure 4C**).

NOTE: Calcein AM marks live cells with green fluorescence (wavelength ~488). EthD-1 represents the signal of dead cells with red fluorescence (wavelength ~594).

7.2.2. Count the number of live and dead cells using imaging software, an open-source image-processing program, and calculate viability with the numbers**.**

8. Immunofluorescence to validate the formation of central hypoxia and its effect on cancer malignancy

8.1. Fixation, permeabilization, and blocking of the cancer construct

8.1.1. Prepare 1x PBS, 4% paraformaldehyde (PFA), 0.1% (v/v) Triton X-100, and 2% (w/v) bovine serum albumin (BSA) at room temperature.

8.1.2. Carefully aspirate all the media from the chip using a pipette and rinse the chip three times with 1x PBS. To avoid deformation of the cancer construct, introduce 1x PBS from one side of the chips and tilt the chips to allow 1x PBS to flow. Between each washing step, let the chip stand with 1x PBS for 5 min to remove residual solutions.

NOTE: 1x PBS was aspirated using a pipette, not a pressure pump.

8.1.3. Add 500 µL of 4% PFA to the cancer construct on the chip using a pipette; leave it for 15 min and wash three times with 1x PBS to fix the cells in the cancer construct.

8.1.4. Treat cancer construct with 500 µL of 0.1% Triton X-100 using a pipette at room temperature for 5 min and wash three times with 1x PBS to solubilize and permeabilize the cell membrane.

8.1.5. Treat cancer construct with 500 µL of 2% BSA using a pipette at room temperature for 1 h to block reactive epitopes.

NOTE: Cover the chip with paraffin film to prevent evaporation.

8.1.6. After 1 h, wash the chip three times with 1x PBS.

8.2. Treatment with primary antibody, secondary antibody, and DAPI and imaging of the structure using a confocal microscope.

8.2.1. Prepare isotype control antibodies and the cocktail of primary antibodies by diluting the antibodies in 1x PBS to each desired working concentration.

NOTE: The specific details of the antibodies are listed in the **Table of Materials**. The same working

concentrations of isotype control antibodies as the primary antibodies should be used.

8.2.2. Carefully aspirate all 1x PBS from the chip using a pipette and treat the chip with 200 µL primary antibody solution at 4 °C overnight. Cover the chips with paraffin film to prevent evaporation.

8.2.3. Aspirate the primary antibody solution and wash the chip three times with 1x PBS.

8.2.4. Dilute secondary antibodies and DAPI in 1x PBS to the desired working concentration.

NOTE: A Green fluorescence-conjugated secondary antibody is used in this case at a ratio of 1:200. DAPI was used at a ratio of 1:1000.

8.2.5. Carefully aspirate all 1x PBS from the chip using a pipette and treat the chip with 200 µL secondary antibody-DAPI solution at 4 °C for 3 h. Cover the chip with paraffin film to prevent evaporation and then wrap it with aluminum foil to prevent photobleaching.

8.2.6. Aspirate the secondary antibody-DAPI solution and wash the chip three times with 1x PBS.

8.2.7. After finishing the staining step, transfer the cancer construct to a confocal dish by gently gripping with forceps.

8.2.8. Visualize and capture the labeled cells using a confocal microscope (**Figure 5**).

NOTE: The wavelength of the confocal microscope was adjusted, depending on the type of the fluorescent markers. The specific details of the antibodies are listed in the **Table of Materials**. To efficiently detect the cell position, it would be better to observe the DAPI stained nuclei of the construct at first. The detection excitation/emission wavelengths of the fluorescent signals were 358/461 nm (DAPI, Blue), 494/517 nm (Green), and 590/617 nm (Red). The magnifications were 4x, 10x, and 20x, adjusted from the lowest to the highest.

9. Statistical analysis

9.1. Cell counting with image processing program

9.1.1. Run an image processing program to count the number of live and dead cells.

9.1.2. Open the fluorescent image files. Click on **File | Open** and import the TIFF images.

9.1.3. Convert the images to 16-bit grayscale images. Click on **Image | Type | 16-bit Grayscale**.

9.1.4. Adjust the threshold by clicking on **Image | Adjust | Threshold** and then select the color of the cells to be black.

9.1.5. Cut merged cells apart by clicking on **Process | Binary | Watershed** for precise cell counting.

9.1.6. Count the number of cells by clicking on **Analyze** and then on **Analyze Particles** three times; calculate the average and present the data as the mean ± standard error.

NOTE: Immunofluorescence markers were analyzed by comparing the fluorescence intensity.

REPRESENTATIVE RESULTS:

The hypoxic cancer-on-a-chip was developed using computer-aided 3D cell-printing technology to recapitulate hypoxia and cancer-related pathology (**Figure 1**). Oxygen transportation and consumption were simulated using the 3D geometry model. The chip was designed in the form of concentric rings to mimic the radial oxygen diffusion and depletion, in cancer tissues (**Figure 2A**). After defining the control volume of a space where oxygen diffused and was consumed by cells, an appropriate cellular density for central hypoxia generation was determined through computational finite element analysis (**Figure 2B,C**).

A 3D printing path code for the hypoxic cancer-on-a-chip was generated based on previous results (**Figure 3**). The CAD files of the sacrificial PEVA mold and cancer constructs were converted to STL file format (**Figure 3A,B**). The printing path was coded and transferred to the multi-printing system using an in-house software program (**Figure 3C**).

A hypoxic cancer-on-a-chip was fabricated using the 3D cell-printing technology. To recapitulate the structural, biochemical, and biophysical heterogeneity of solid cancer, a stepwise fabrication process was established for the cancer construct and the gas-permeable barrier, which is the only manner in which oxygen can penetrate the system (**Figure 4A**). A compartmentalized cancer-stroma concentric-ring structure was created to reproduce the anatomical features of the solid cancer (**Figure 4B**). The heterogeneous geometry of the cancer tissue was realized in vitro using the 3D cell-printing technology. Cell viability was evaluated after printing to confirm the chemical and mechanical stress during the fabrication process. The ratio of the green-stained live cells was significantly higher than that of the red-stained dead cells. Quantitatively, the post-printing cell viability was more than 96.92% ± 2.46% (**Figure 4C**). This result confirms that the manufacturing conditions were appropriate for cancer cells and stromal cells.

Two groups were compared depending on the presence (GR^+) and absence (GR^-) of the oxygen gradient to verify the effects of the hypoxic gradient on cancer progression (**Figure 5A**). Under both conditions, matured $CD31^+$ endothelial cells existed in the peripheral regions, which indicated that spatially patterned living construct was produced using 3D bioprinting technology. Compared with the GR^- condition, the GR^+ condition showed a hypoxic gradient, indicating the gradual expression of HIF1α (**Figure 5B**), where $SHMT2^+$ pseudopalisading cells and $SOX2^+$ pluripotent cells were observed, which represented the aggressive pathophysiological feature of solid cancer (**Figure 5C**). Namely, the pathological features of glioblastoma were recapitulated under the engineered hypoxic condition[15].

FIGURES AND TABLES:

FIGURE AND TABLE LEGENDS:

Figure 1: A schematic of the development of hypoxic cancer-on-a-chip. This figure has been modified from Nature biomedical engineering[15] (Copyright, 2019).

Figure 2: Computational simulation of formation of oxygen gradient on hypoxic cancer on-a-chip. (**A**) A 3D geometry of hypoxic cancer-on-a-chip. (**B**) A schematic indicating the region for oxygen distribution analysis. This figure has been modified from Nature biomedical engineering[15] (Copyright, 2019). (**C**) A jet color map image of the oxygen distribution profile. This figure has been modified from Nature biomedical engineering[15] (Copyright, 2019).

Figure 3: Generation of 3D printing path code for hypoxic cancer-on-a-chip. (**A**) A 3D geometry of sacrificial PEVA mold. (**B**) An image of sacrificial PEVA mold in STL file format. (**C**) A G-code of sacrificial PEVA mold.

Figure 4: 3D cell-printing of hypoxic cancer-on-a-chip. (**A**) A schematic of the fabrication process of hypoxic cancer-on-a-chip. (**B**) A printed hypoxic cancer-on-a-chip and compartmentalized structure of cancer-stroma concentric rings; scale bars represent 200 μm. (**C**) A fluorescence image of the 3D cell-printed cancer construct for evaluating viability; scale bars represent 200 μm.

Figure 5: Generation of hypoxic gradient and evaluation of pathological features of engineered solid cancer. (**A**) Experimental groups under two different oxygen permeability conditions. (**B**) Representative immunostaining images of generation of oxygen gradient using HIF1α; scale bars represent 200 μm. (**C**) Representative immunostaining images of pathological features of hypoxic cancer using SHMT2, SOX2, and CD31; scale bars represent 200 μm. This figure has been modified from Nature biomedical engineering[15] (Copyright, 2019).

DISCUSSION:

In this study, we describe the fabrication process of a hypoxic cancer-on-a-chip based on 3D cell-printing technology. The formation of the hypoxic gradient in the designed chip was predicted through computer simulations. The environment that can induce a heterogeneous hypoxic gradient was reproduced via a simple strategy combining the 3D-printed gas-permeable barrier and the glass cover. The hypoxia-related pathological features of glioblastoma, including pseudopalisade and a small population of cancer stem cells, were recapitulated under hypoxic gradient conditions of the chip.

To improve productivity and repeatability, two major fabrication steps were sequentially modified compared with the previously published model[15]. First, a PDMS barrier was produced indirectly to overcome the poor printability of PDMS containing a curing agent, which is cured in real time rather than through a one-step-direct printing method. Therefore, biocompatible PEVA having higher printability was adapted to fabricate the sacrificial mold and PDMS was added to

create the gas-permeable barrier. Second, the type of slide glass was changed into a hydrophilic-coated slide glass, which is favorable to support bioink deposition and shape fidelity. Finally, building the medium reservoirs at both ends of the chip efficient medium exchange was made possible.

Critical factors in each fabrication step of hypoxic cancer-on-a-chip via 3D bioprinting should be cautiously controlled. During casting, the height of PDMS should be greater than that of the sacrificial PEVA mold, otherwise the chip tightened with the cover glass becomes loose, which has a negative effect on hypoxic core generation. During printing of collagen, a thermally sensitive hydrogel, the temperature of the printing head should be maintained at 15 ˚C to prevent the nozzle clogging due to a sol-gel transition phenomenon. If the hydrogel becomes temporally cross-linked, the blocked nozzle can be easily cleaned using a high pneumatic pressure and a sharp needle. However, if the blocking is severe, the hydrogel should be prepared again. Furthermore, the cell-printing process should be completed within 1 h, considering cell viability.

The 3D bioprinting technology facilitates the engineering of a hypoxic cancer-on-a-chip that can be used to study the underlying mechanism of cancer and to predict the therapeutic resistance of various solid tumors[15]. Especially, the use of extrusion-based 3D bioprinting technology enabled rapid and repetitive production with a high level of freedom. Furthermore, the reproducibility and fast time frame for cancer modeling allow the pharmaceutical field to build a dataset of drug combination candidates for cancer treatment. However, due to the limited resolution of the technology, the printed hypoxic-cancer-on-a-chip is produced in the range of several hundred micrometers, requiring large amount of materials. In addition, it is difficult to develop high throughput drug screening platform under the space restraints[20]. Therefore, the technology should be improved to develop models capable of supporting multiparameter studies with limited resources and spatial extent.

The developed hypoxic-cancer-on-a-chip can be applied to tissue-specific cancer modeling by employing tissue-specific materials, such as a hydrogel derived from a decellularized extracellular matrix (ECM). Because the biochemical and physiological variations of the ECM affect cellular functions, superior emulation of numerous cancer types with an organ-specific cancer microenvironment can be realized[21]. In addition, by combining with other engineered tissue constructs, including engineered blood vessels, that have critical impacts on cancer development, dynamic pathophysiological changes in angiogenic, immunogenic, and metastatic properties can be studied. Furthermore, personalized cancer therapy can be accomplished with the developed chip by employing patient-derived cells[15]. Testing drug sensitivity prior to clinical treatment would be a significant step to improve the efficacy of the therapy during the process of finding an appropriate therapeutic regimen for an individual patient in time. A patient-specific cancer model with a patient-derived source is expected to improve the patient profiling to predict differences in pathophysiology and chemosensitivity of each patient. In the previous study, patient-specific therapeutic effects against various drug combinations were predicted within a reasonable timeframe (1–2 weeks) using the 3D printed hypoxic cancer-on-a-chip, which results in relatively quick conclusions compared to other methods, suggesting the potential for the patient-specific preclinical model[15].

In summary, 3D cell-printing of cancer-on-a-chip is favorable for recapitulating a heterogeneous cancer microenvironment. The mimicked microenvironment drives the pathological progression of cancer, including the formation of a necrotic core resulting from hypoxia. This protocol can be applied to anticancer drug testing and patient-specific cancer models. In this regard, we expect that this highly controllable approach may be beneficial for building various cancer models.

ACKNOWLEDGMENTS:

This research was supported by the National Research Foundation of Korea (NRF) funded by the Ministry of Education (No. 2020R1A6A1A03047902) and the Korea government (MSIT) (No. NRF-2019R1C1C1009606, NRF-2019R1A3A3005437, and NRF-2018H1A2A1062091).

DISCLOSURES:

The authors have no disclosures.

REFERENCES:

1. Jing, X. et al. Role of hypoxia in cancer therapy by regulating the tumor microenvironment. *Molecular Cancer*. **18** (1), 157 (2019).
2. Al Tameemi, W., Dale, T. P., Al-Jumaily, R. M. K., Forsyth, N. R. Hypoxia-modified cancer cell metabolism. *Frontiers in Cell and Developmental Biology*. **7**, 4 (2019).
3. Petrova, V., Annicchiarico-Petruzzelli, M., Melino, G., Amelio, I. The hypoxic tumour microenvironment. *Oncogenesis*. **7** (1), 1–13 (2018).
4. Hockel, M., Vaupel, P. Tumor hypoxia: definitions and current clinical, biologic, and molecular aspects. *Journal of the National Cancer Institute*. **93** (4), 266–276 (2001).
5. Kim, H., Lin, Q., Glazer, P. M., Yun, Z. The hypoxic tumor microenvironment in vivo selects the cancer stem cell fate of breast cancer cells. *Breast Cancer Research*. **20** (1), 16 (2018).
6. Jeong, G. S., Lee, J., Yoon, J., Chung, S., Lee, S.-H. Viscoelastic lithography for fabricating self-organizing soft micro-honeycomb structures with ultra-high aspect ratios. *Nature Communications*. **7** (1), 1–9 (2016).
7. Razian, G., Yu, Y., Ungrin, M. Production of large numbers of size-controlled tumor spheroids using microwell plates. *Journal of Visualized Experiments: JoVE*. (81), e50665 (2013).
8. Nunes, A. S., Barros, A. S., Costa, E. C., Moreira, A. F., Correia, I. J. 3D tumor spheroids as in vitro models to mimic in vivo human solid tumors resistance to therapeutic drugs. *Biotechnology and Bioengineering*. **116** (1), 206–226 (2019).
9. Wan, L., Neumann, C., LeDuc, P. Tumor-on-a-chip for integrating a 3D tumor microenvironment: chemical and mechanical factors. *Lab on a Chip*. **20** (5), 873–888 (2020).
10. Nam, H., Funamoto, K., Jeon, J. S. Cancer cell migration and cancer drug screening in oxygen tension gradient chip. *Biomicrofluidics*. **14** (4), 044107 (2020).
11. Palacio-Castañeda, V., Kooijman, L., Venzac, B., Verdurmen, W. P., Le Gac, S. Metabolic switching of tumor cells under hypoxic conditions in a tumor-on-a-chip model. *Micromachines*. **11** (4), 382 (2020).
12. Ronaldson-Bouchard, K., Vunjak-Novakovic, G. Organs-on-a-chip: a fast track for engineered human tissues in drug development. *Cell Stem Cell*. **22** (3), 310–324 (2018).
13. Mi, S., Du, Z., Xu, Y., Sun, W. The crossing and integration between microfluidic technology

and 3D printing for organ-on-chips. *Journal of Materials Chemistry B*. **6** (39), 6191–6206 (2018).
14. Yi, H.-G., Lee, H., Cho, D.-W. 3D printing of organs-on-chips. *Bioengineering*. **4** (1), 10 (2017).
15. Yi, H.-G. et al. A bioprinted human-glioblastoma-on-a-chip for the identification of patient-specific responses to chemoradiotherapy. *Nature Biomedical Engineering*. **3** (7), 509–519 (2019).
16. Kang, T.-Y., Hong, J. M., Jung, J. W., Yoo, J. J., Cho, D.-W. Design and assessment of a microfluidic network system for oxygen transport in engineered tissue. *Langmuir*. **29** (2), 701–709, (2013).
17. Woo Jung, J. et al. Evaluation of the effective diffusivity of a freeform fabricated scaffold using computational simulation. *Journal of Biomechanical Engineering*. **135** (8) (2013).
18. Brown, A. C., De Beer, D. Development of a stereolithography (STL) slicing and G-code generation algorithm for an entry level 3-D printer. *2013 Africon* (IEEE). 1–5 (2013).
19. Shim, J.-H., Lee, J.-S., Kim, J. Y., Cho, D.-W. Bioprinting of a mechanically enhanced three-dimensional dual cell-laden construct for osteochondral tissue engineering using a multi-head tissue/organ building system. *Journal of Micromechanics and Microengineering*. **22** (8), 085014 (2012).
20. Gillispie, G. et al. Assessment methodologies for extrusion-based bioink printability. *Biofabrication*. **12** (2), 022003 (2020).
21. Kim, B. S., Das, S., Jang, J., Cho, D.-W. Decellularized extracellular matrix-based bioinks for engineering tissue-and organ-specific microenvironments. *Chemical Reviews*. **120** (19), 10608–10661 (2020).

Figure 1

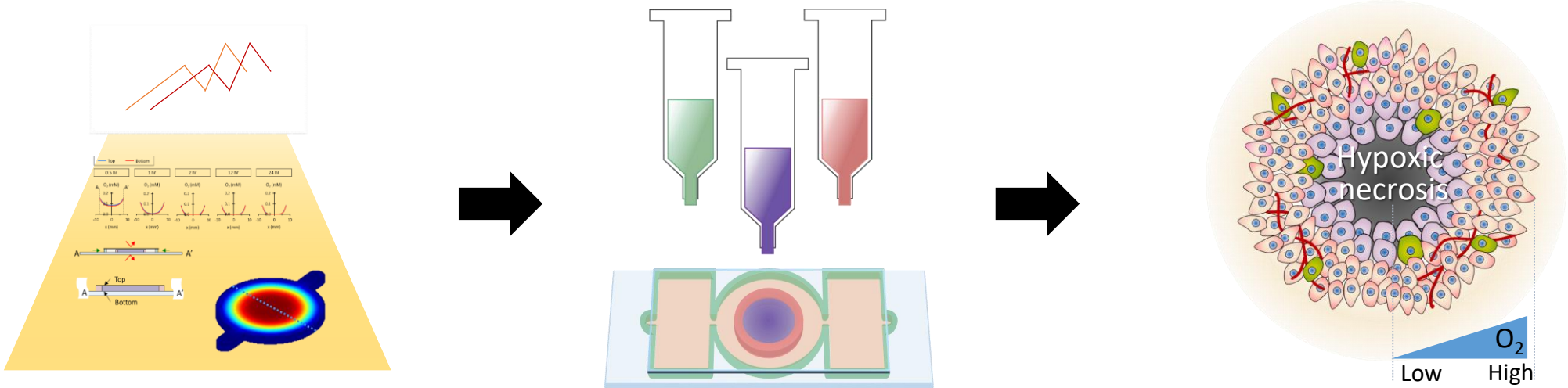

Computational simulation of oxygen gradient formation

3D cell-printing of solid-cancer-on-a-chip

Generation of hypoxic gradient and evaluation of pathologic features

Figure 2

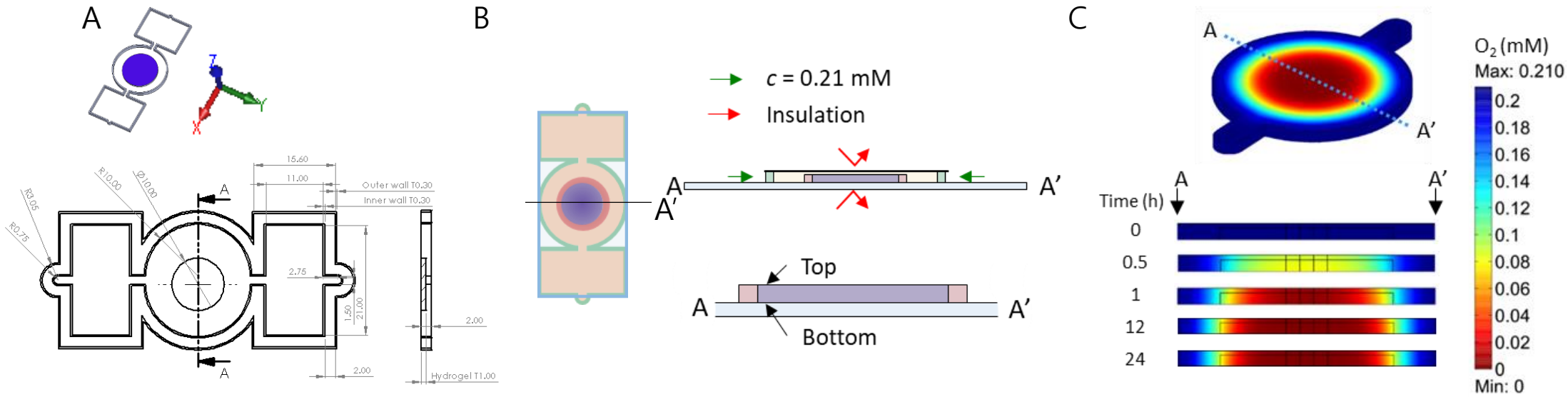

Figure 3

A

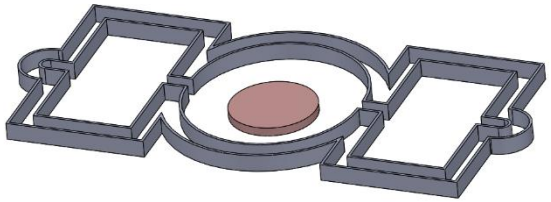

B

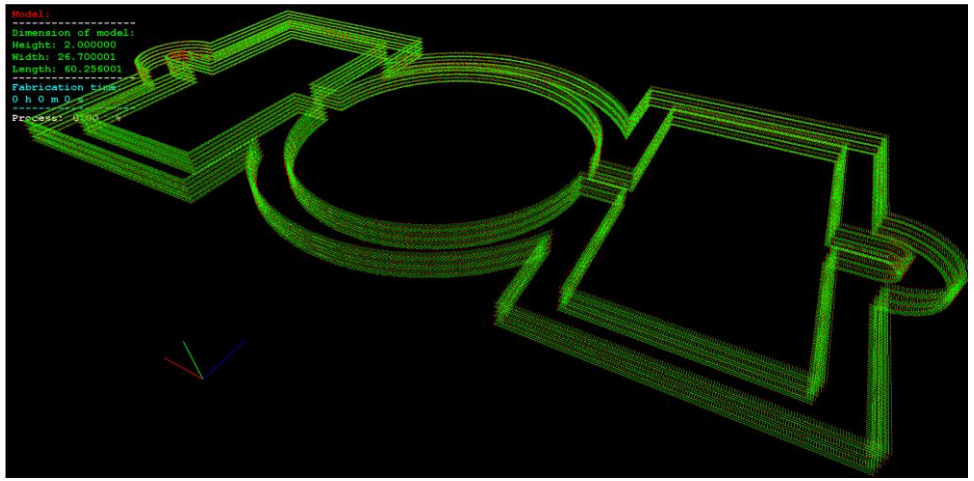

C

```
T4 M06
M84
G91
G01 Z20.0 F401
G01 Y34.0 F401
G01 X-10.00 F401
G01 Z-19.00 F401

M16
G04 X0.5

;***********************************************
G01 X-2.750 Y0.000 F401
G01 X0 Y9.250 F401
G01 X-11 Y0.000 F401
G01 X0 Y-9.250 F401
G01 X-3.028 Y0.000 F401
G03 X-20.04 Y0.0 R10.08 F401
;G03 X-20.04 Y0.0 R10.08 F401
G01 X-3.028 Y0.000 F401
G01 X0 Y9.250 F401
G01 X-11 Y0.000 F401
G01 X0 Y-9.250 F401
G01 X-2.750 Y0.000 F401
G03 X0.000 Y-1.500 R0.750 F201
G01 X2.750 Y0.000 F401
G01 X0 Y-9.250 F401
G01 X11.000 Y0.000 F401
G01 X0.000 Y9.250 F401
G01 X3.028 Y0.000 F401
G03 X20.04 Y0.0 R10.08 F401
G01 X3.028 Y0.000 F401
G01 X0 Y-9.250 F401
G01 X11.000 Y0.000 F401
G01 X0.000 Y9.250 F401
G01 X2.750 Y0.000 F401
G03 X0.000 Y1.500 R0.750 F201
```

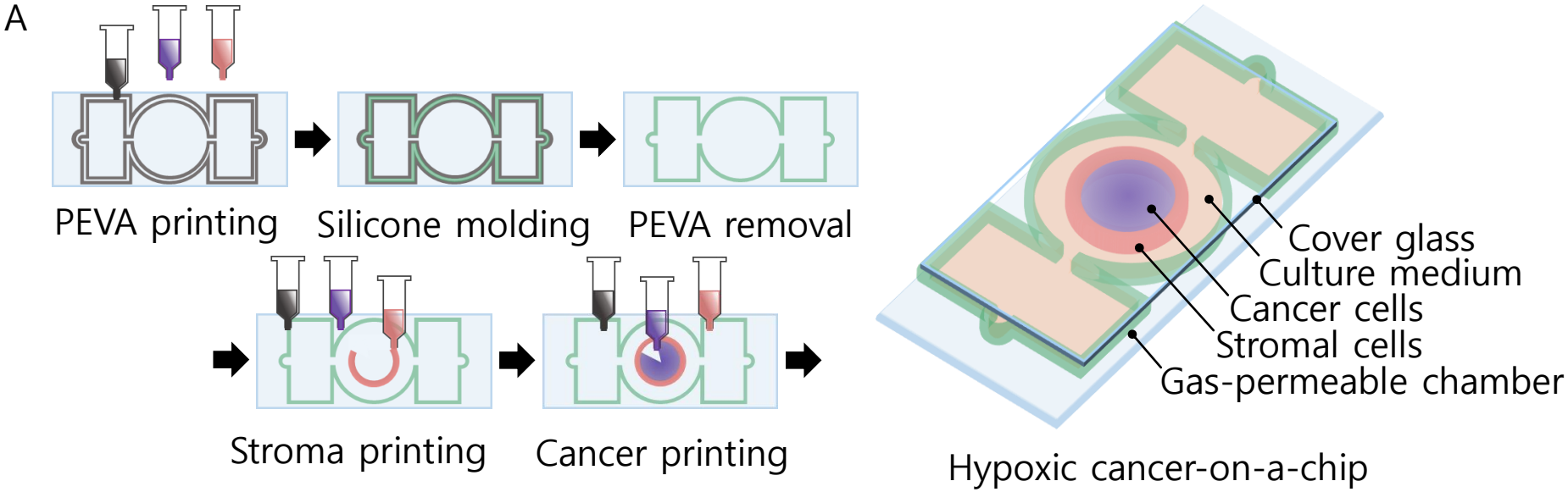

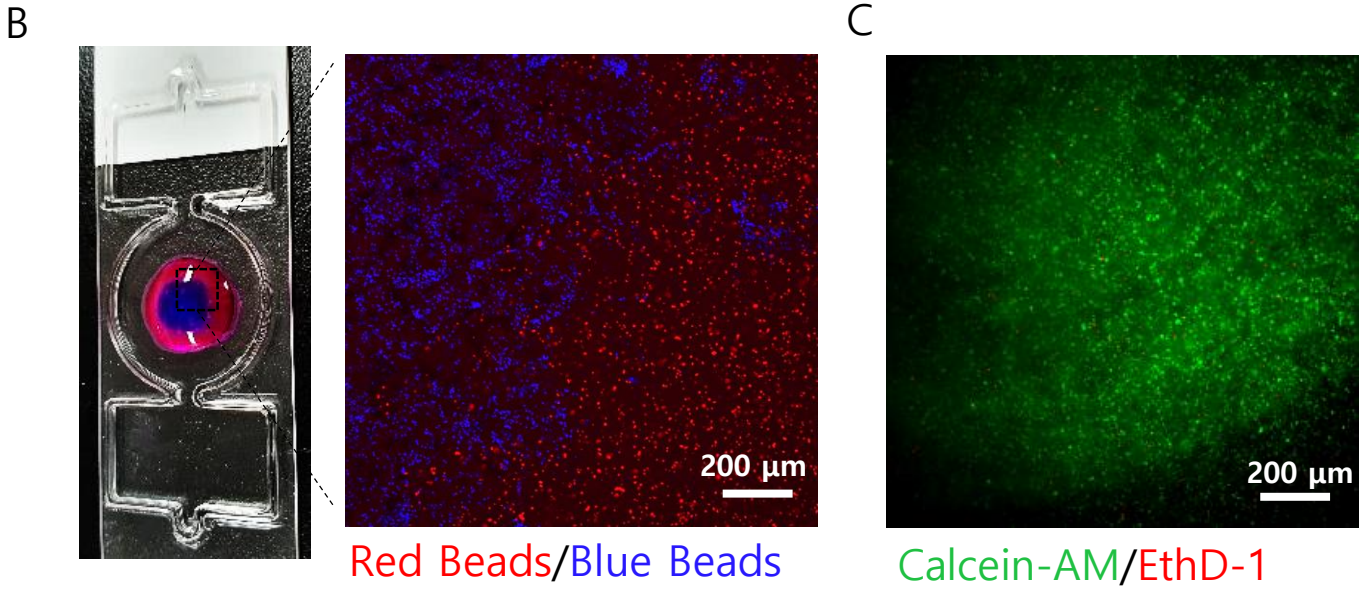

Figure 5

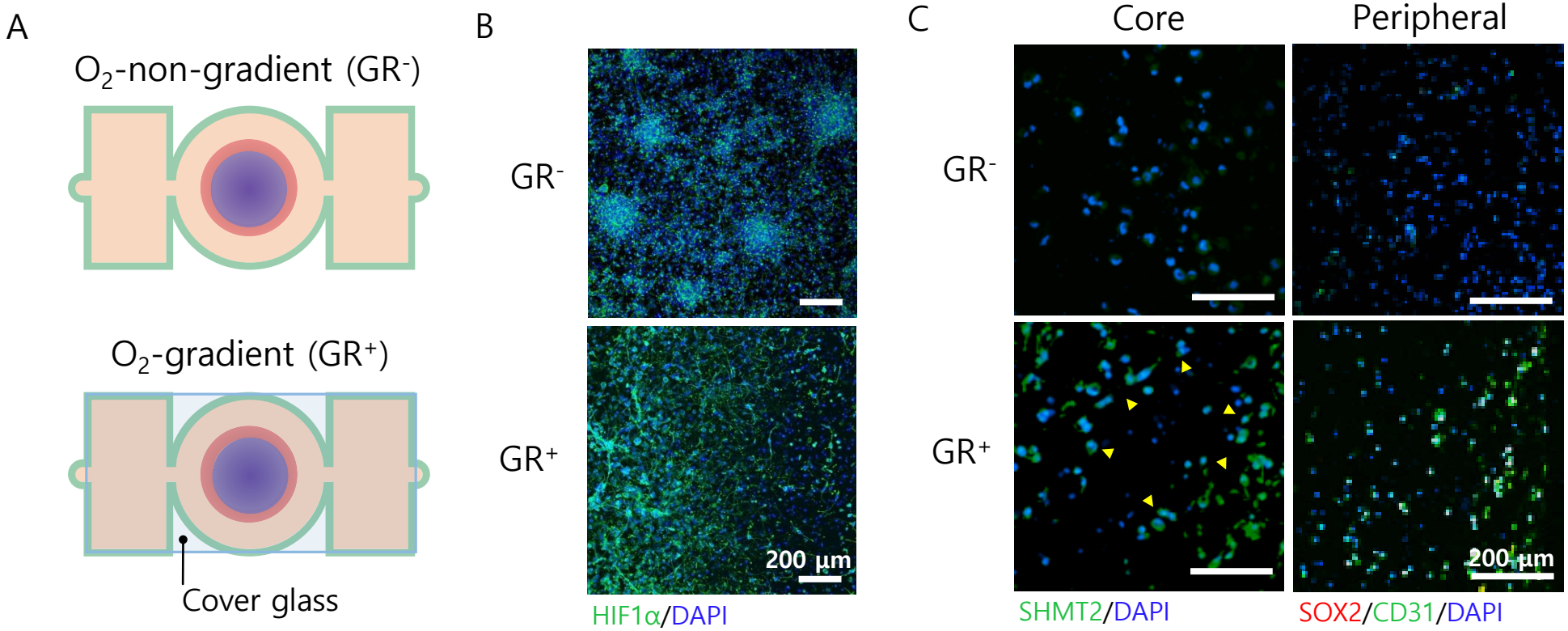

Table of Materials

Click here to access/download;Table of Materials;JoVE_Table_of_Materials_R2.xlsx

Name of Material/Equipment	Company	Catalog Number	Comments/Description
Cells			
Human umbilical vein endothelial cells	Promocell	C-12200	
U-87 MG cells	ATCC	ATCC HTB-14	
Disposable			
0.2 µm syringe filter	Sartorius	16534-K	
10 mL disposable syringe	Jung Rim	10ml 21G32	
10 mL glass vial	Hubena	A0039	
10 mL Serological pipette tip	SPL lifescience	91010	
15 mL conical tube	SPL lifescience	50015	
18G plastic needle	Musashi engineering	PN-18G-B	
20G plastic tapered dispense tip	Musashi engineering	TPND-20G-U	
22x50 glass cover	MARIENFIELD	0101142	
25 mL Serological pipette tip	SPL lifescience	90125	
3 mL disposable syringes	HENKE-JET	4020-X00V0	
40 µm cell strainer	Falcon	352360	
5 mL Serological pipette tip	SPL lifescience	91005	
50 mL conical tube	SPL lifescience	50050	
50 mL Serological pipette tip	SPL lifescience	90150	
50N precision nozzle	Musashi engineering	HN-0.5ND	
Aluminum foil	SINKWANG		
Capillary tips	Gilson	CP1000	
Cell-scrapper	SPL lifescience	90030	
Confocal dish	SPL lifescience	200350	
Parafilm	Bemis	PM996	
Pre-coated histology slide	MATSUNAMI	MAS-11	
Reservoir	SPL lifescience	23050	
T-75 cell culture flask	SPL lifescience	70075	
Equipment			
3DX printer	T&R Biofab		
Autoclave	JEIOTECH	AC-12	
Centrifuger	Cyrozen	1580MGR	

Confocal laser microscopy	Olympus Life Science	FV 1000	
Fluorescence microscope	FISHER SCEINTIFIC	O221S366	
Forcep	Korea Ace Scientific	HC.203-30	
Hand tally counter	KTRIO		
Hemocytometer	MARIENFIELD	0650030	
Incubator	Panasonic	MCO-170AIC	
Laminar flow cabinet	DAECHUNG SCIENCE	CB-BMMS C-001	
Metal syringe	IWASHITA engineering	SUS BARREL 10CC	
Operating Scissors	Hirose	HC.13-122	
Oven	JEIOTECH	OF-12, H070023	
Positive displacement pipette	GILSON	NJ05652	
Refrigerator	SAMSUNG	CRFD-1141	
Voltex Mixer	DAIHAN scientific	VM-10	
Water bath	DAIHAN SCIENTIFIC	WB-11	
Water purifier	WASSER LAB	DI-GR	
Materials			
0.25 % Trypsin-EDTA	Gibco	25200-072	
10x PBS	Intron	IBS-BP007a	
4% Paraformaldehyde	Biosesang		
70% Ethanol	Daejung	4018-4410	
Anti-CD31 antibody	Abcam	ab28364	
Anti-HIF-1 alpha antibody	Abcam	ab16066	
Anti-SHMT2/SHMT antibody	Abcam	ab88664	
Anti-SOX2 antibody	Abcam	ab75485	
Bovine Serum Albumin	Thermo scientific	J10857-22	
Collagen from porcine skin	Dalim tissen	PC-001-1g	
DAPI (4',6-Diamidino-2-Phenylindole, Dihydrochloride)	Thermofisher	D1306	
Endothelial Cell Growth Medium-2	Promocell	C22011	
Fetal bovine serum	Gibco	12483-020	
Goat anti-Mouse IgG (H+L) Cross-Adsorbed Secondary Antibody, Alexa Fluor 488	Theromofisher	A-11001	
Goat anti-Rabbit IgG (H+L) Cross-Adsorbed Secondary Antibody, Alexa Fluor 594	Theromofisher	A-11012	

High-glucose Dulbecco's Modified Eagle Medium(DMEM)	Hyclone	SH30243-0	
Hydrochloric acid	Sigma-Aldrich	311413-100ML	
Live/dead assay kit	Invitrogen	L3224	
Mouse IgG1, kappa monoclonal [15-6E10A7] - Isotype Control	Abcam	ab170190	
Penicillin/streptomycin	Gibco	15140-122	
Phenol red solution	Sigma-Aldrich	P0290-100ML	
Poly(ethylene-vinyl acetate)	Poly science	06108-500	
Polydimethylsiloxane	Dowhitech	sylgard 184	
Rabbit IgG, polyclonal - Isotype Control	Abcam	ab37415	
Sodium hydroxide solution	Samchun	S0610	
Triton X-100	Biosesang	TRI020-500-50	
Trypan Blue	Sigma-Aldrich	T8154	
Software			
COMSOL Multiphysics 3.5a	COMSOL AB		
IMS beamer			in-house software
SolidWorks Package	Dassault Systems SolidWorks Corporation		

Response to Editorial Comments

Manuscript ID	JoVE61945
Title	3D Cell-Printed Hypoxic Cancer-on-a-Chip for Recapitulating Pathologic Progression of Solid Cancer
Authors	Wonbin Park, Mihyeon Bae, Minseon Hwang, Jinah Jang, Dong-Woo Cho, Hee-Gyeong Yi

Editor's comment 1:

The editor has formatted the manuscript to match the journal's style. Please retain and use the attached file for revision.

Response 1:

The authors would like to thank editor for taking the time to read the manuscript and for the valuable remarks.

Editor's comment 2:

Please address all the specific comments marked in the manuscript.

Response 2:

Thank you for your valuable comments. We revised the manuscript according to your comments and highlighted in red. Please check the revised manuscript. For your information, the replies for each comment are highlighted in blue.

Editor's comment 3:

Once done please ensure that the protocol highlight is no more than 3 pages including headings and spacings.

Response 3:

According to the editor's comment, we have highlighted the part in yellow within 3 pages.

Editor's comment 4:

Please proofread the manuscript well before submission.

Response 4:

According to editor's comment, we thoroughly proofread the manuscript to ensure that there are no spelling or grammar issues.

SPRINGER NATURE LICENSE
TERMS AND CONDITIONS

Oct 26, 2020

This Agreement between Ms. Wonbin Park ("You") and Springer Nature ("Springer Nature") consists of your license details and the terms and conditions provided by Springer Nature and Copyright Clearance Center.

All payments must be made in full to CCC. For payment instructions, please see information listed at the bottom of this form.

License Number	4932970592661
License date	Oct 20, 2020
Licensed Content Publisher	Springer Nature
Licensed Content Publication	Nature Biomedical Engineering
Licensed Content Title	A bioprinted human-glioblastoma-on-a-chip for the identification of patient-specific responses to chemoradiotherapy
Licensed Content Author	Hee-Gyeong Yi et al
Licensed Content Date	Mar 18, 2019
Type of Use	Journal/Magazine
Requestor type	non-commercial (non-profit)
Is this reuse sponsored by or associated with a pharmaceutical or a medical products company?	no
Format	print and electronic

Portion	figures/tables/illustrations
Number of figures/tables/illustrations	3
High-res required	yes
Will you be translating?	no
Circulation/distribution	1 - 29
Author of this Springer Nature content	yes
Title of new article	3D Cell-Printed Hypoxic Cancer-on-a-Chip for Recapitulating Pathologic Progression of Solid Cancer
Lead author	Wonbin Park, Mihyeon Bae
Title of targeted journal	Jove
Publisher	Jove
Expected publication date	Jun 2021
Portions	Figure 3a, 3d, Supplementary figure 2b, 2d, 4d
Requestor Location	Ms. Wonbin Park 77 Cheongam-ro, Nam-gu Pohang, 790-784 Korea, Republic Of Attn: Ms. Wonbin Park
Billing Type	Credit Card
Credit card info	Master Card ending in 3038
Credit card expiration	03/2024

Total 271.40 USD

Terms and Conditions

Springer Nature Customer Service Centre GmbH
Terms and Conditions

This agreement sets out the terms and conditions of the licence (the **Licence**) between you and **Springer Nature Customer Service Centre GmbH** (the **Licensor**). By clicking 'accept' and completing the transaction for the material (**Licensed Material**), you also confirm your acceptance of these terms and conditions.

1. Grant of License

1. 1. The Licensor grants you a personal, non-exclusive, non-transferable, world-wide licence to reproduce the Licensed Material for the purpose specified in your order only. Licences are granted for the specific use requested in the order and for no other use, subject to the conditions below.

1. 2. The Licensor warrants that it has, to the best of its knowledge, the rights to license reuse of the Licensed Material. However, you should ensure that the material you are requesting is original to the Licensor and does not carry the copyright of another entity (as credited in the published version).

1. 3. If the credit line on any part of the material you have requested indicates that it was reprinted or adapted with permission from another source, then you should also seek permission from that source to reuse the material.

2. Scope of Licence

2. 1. You may only use the Licensed Content in the manner and to the extent permitted by these Ts&Cs and any applicable laws.

2. 2. A separate licence may be required for any additional use of the Licensed Material, e.g. where a licence has been purchased for print only use, separate permission must be obtained for electronic re-use. Similarly, a licence is only valid in the language selected and does not apply for editions in other languages unless additional translation rights have been granted separately in the licence. Any content owned by third parties are expressly excluded from the licence.

2. 3. Similarly, rights for additional components such as custom editions and derivatives require additional permission and may be subject to an additional fee. Please apply to Journalpermissions@springernature.com/bookpermissions@springernature.com for these rights.

2. 4. Where permission has been granted **free of charge** for material in print, permission may also be granted for any electronic version of that work, provided that the material is incidental to your work as a whole and that the electronic version is essentially equivalent to, or substitutes for, the print version.

2. 5. An alternative scope of licence may apply to signatories of the STM Permissions Guidelines, as amended from time to time.

3. Duration of Licence

3. 1. A licence for is valid from the date of purchase ('Licence Date') at the end of the relevant period in the below table:

Scope of Licence	Duration of Licence
Post on a website	12 months
Presentations	12 months
Books and journals	Lifetime of the edition in the language purchased

4. Acknowledgement

4. 1. The Licensor's permission must be acknowledged next to the Licenced Material in print. In electronic form, this acknowledgement must be visible at the same time as the figures/tables/illustrations or abstract, and must be hyperlinked to the journal/book's homepage. Our required acknowledgement format is in the Appendix below.

5. Restrictions on use

5. 1. Use of the Licensed Material may be permitted for incidental promotional use and minor editing privileges e.g. minor adaptations of single figures, changes of format, colour and/or style where the adaptation is credited as set out in Appendix 1 below. Any other changes including but not limited to, cropping, adapting, omitting material that affect the meaning, intention or moral rights of the author are strictly prohibited.

5. 2. You must not use any Licensed Material as part of any design or trademark.

5. 3. Licensed Material may be used in Open Access Publications (OAP) before publication by Springer Nature, but any Licensed Material must be removed from OAP sites prior to final publication.

6. Ownership of Rights

6. 1. Licensed Material remains the property of either Licensor or the relevant third party and any rights not explicitly granted herein are expressly reserved.

7. Warranty

IN NO EVENT SHALL LICENSOR BE LIABLE TO YOU OR ANY OTHER PARTY OR ANY OTHER PERSON OR FOR ANY SPECIAL, CONSEQUENTIAL, INCIDENTAL OR INDIRECT DAMAGES, HOWEVER CAUSED, ARISING OUT OF OR IN CONNECTION WITH THE DOWNLOADING, VIEWING OR USE OF THE MATERIALS REGARDLESS OF THE FORM OF ACTION, WHETHER FOR BREACH OF CONTRACT, BREACH OF WARRANTY, TORT, NEGLIGENCE, INFRINGEMENT OR OTHERWISE (INCLUDING, WITHOUT LIMITATION, DAMAGES BASED ON LOSS OF PROFITS, DATA, FILES, USE, BUSINESS OPPORTUNITY OR CLAIMS OF

THIRD PARTIES), AND
WHETHER OR NOT THE PARTY HAS BEEN ADVISED OF THE POSSIBILITY OF SUCH DAMAGES. THIS LIMITATION SHALL APPLY NOTWITHSTANDING ANY FAILURE OF ESSENTIAL PURPOSE OF ANY LIMITED REMEDY PROVIDED HEREIN.

8. Limitations

8. 1. ***BOOKS ONLY:***Where **'reuse in a dissertation/thesis'** has been selected the following terms apply: Print rights of the final author's accepted manuscript (for clarity, NOT the published version) for up to 100 copies, electronic rights for use only on a personal website or institutional repository as defined by the Sherpa guideline (www.sherpa.ac.uk/romeo/).

9. Termination and Cancellation

9. 1. Licences will expire after the period shown in Clause 3 (above).

9. 2. Licensee reserves the right to terminate the Licence in the event that payment is not received in full or if there has been a breach of this agreement by you.

Appendix 1 — Acknowledgements:

For Journal Content:
Reprinted by permission from [**the Licensor**]: [**Journal Publisher** (e.g. Nature/Springer/Palgrave)] [**JOURNAL NAME**] [**REFERENCE CITATION** (Article name, Author(s) Name), [**COPYRIGHT**] (year of publication)

For **Advance Online Publication papers:**
Reprinted by permission from [**the Licensor**]: [**Journal Publisher** (e.g. Nature/Springer/Palgrave)] [**JOURNAL NAME**] [**REFERENCE CITATION** (Article name, Author(s) Name), [**COPYRIGHT**] (year of publication), advance online publication, day month year (doi: 10.1038/sj.[JOURNAL ACRONYM].)

For Adaptations/Translations:
Adapted/Translated by permission from [**the Licensor**]: [**Journal Publisher** (e.g. Nature/Springer/Palgrave)] [**JOURNAL NAME**] [**REFERENCE CITATION** (Article name, Author(s) Name), [**COPYRIGHT**] (year of publication)

Note: For any republication from the British Journal of Cancer, the following credit line style applies:

Reprinted/adapted/translated by permission from [**the Licensor**]: on behalf of Cancer Research UK: : [**Journal Publisher** (e.g. Nature/Springer/Palgrave)] [**JOURNAL NAME**] [**REFERENCE CITATION** (Article name, Author(s) Name), [**COPYRIGHT]** (year of publication)

For **Advance Online Publication** papers:
Reprinted by permission from The [**the Licensor**]: on behalf of Cancer Research UK: [**Journal Publisher** (e.g. Nature/Springer/Palgrave)] [**JOURNAL NAME**] [**REFERENCE CITATION** (Article name, Author(s) Name), [**COPYRIGHT**] (year

of publication), advance online publication, day month year (doi: 10.1038/sj.[JOURNAL ACRONYM])

For Book content:
Reprinted/adapted by permission from [**the Licensor**]: [**Book Publisher** (e.g. Palgrave Macmillan, Springer etc) [**Book Title**] by [**Book author**(s)] [**COPYRIGHT**] (year of publication)

Other Conditions:

Version 1.2

Questions? customercare@copyright.com or +1-855-239-3415 (toll free in the US) or +1-978-646-2777.